Stoch Environ Res Risk Assess (2011) 25:35–49
DOI 10.1007/s00477-010-0435-7

ORIGINAL PAPER

Evaluation of dam overtopping probability induced by flood and wind

Yung-Chia Hsu · Yeou-Koung Tung · Jan-Tai Kuo

Published online: 17 September 2010

Abstract This study develops a probability-based methodology to evaluate dam overtopping probability that accounts for the uncertainties arising from wind speed and peak flood. A wind speed frequency model and flood frequency analysis, including various distribution types and uncertainties in their parameters, are presented. Furthermore, dam overtopping probabilities based on monthly maximum (MMax) series models are compared with those of the annual maximum (AMax) series models. An efficient sampling scheme, which is a combination of importance sampling (IS) and Latin Hypercube sampling (LHS) methods, is proposed to generate samples of peak flow rate and wind speed especially for rare events. Reservoir routing, which incorporates operation rules, wind setup, and run-up, is used to evaluate dam overtopping probability.

Keywords Dam overtopping · Flood frequency · Sampling method · Frequency model

Y.-C. Hsu (✉)
Disaster Prevention and Water Environment Research Center, National Chiao Tung University, Hsinchu, Taiwan
e-mail: ychsu1978@gmail.com

Y.-K. Tung
Department of Civil and Environmental Engineering, The Hong Kong University of Science and Technology, Clear Water Bay, Kowloon, Hong Kong

J.-T. Kuo
Department of Civil Engineering, National Taiwan University, Taipei, Taiwan

1 Introduction

Taiwan, located in Southeast Asia, is frequently visited by typhoons and earthquakes. The general public is more and more concerned with dam safety issue. According to the International Commission on Large Dams (ICOLD 1973), overtopping constitutes about 35% of all earth dam failures; seepage, piping and other causes make up the rest. Various studies have proposed procedures for dam safety assessments (Langseth and Perkins 1983; Karlsson and Haimes 1988a, b; Haimes 1988; Karlsson and Haimes 1989; Von Thun 1987). The National Research Council (NRC 1988) of USA has proposed general approaches to evaluate probability distributions associated with extreme precipitation and runoff. There are two sources of error associated with estimated quantiles from frequency analysis. The first type arises from the assumption that the observations follow a particular distribution; the second type is the error inherent in parameter estimates from limited samples. The uncertainties associated with flood quantile of any return period and adopted distributions would affect dam overtopping probability.

In earlier studies (Askew et al. 1971; Cheng et al. 1982; Afshar and Marino 1990; Meon 1992; Pohl 1999; Kwon and Moon 2006; Kuo et al. 2007, 2008), dam overtopping probability was assessed without considering the possible errors arising from adopting a particular distribution model for flood data or the uncertainty of estimated flood quantiles. Therefore, this study takes into account the two types of errors and proposes a sampling scheme that combines the importance sampling (IS) and the Latin hypercube sampling (LHS) for generating random floods and wind speeds in dam safety evaluation.

Risk and uncertainty analysis methods have been conducted on safety assessments of hydraulic infrastructural

systems for years. Tung and Mays (1981) applied the first-order second-moment (FOSM) method to flood levee design. Hsu et al. (2007) presents a solution by projecting FOSM results to obtain an equivalent most probable failure point in the material space as defined by the advanced first-order second-moment (AFOSM). Cheng et al. (1982) and Cheng (1993) applied the AFOSM method for dam overtopping assessment. Yeh and Tung (1993) applied the FOSM method to evaluate the uncertainty and sensitivity of a pit-migration model for sand and gravel mining from riverbed. Askew et al. (1971) used Monte Carlo sampling (MCS) technique to evaluate the design of a multi-object reservoir system. McKay (1988) developed the LHS method, and it was proved to achieve a convergence in system performance more quickly with less samples than the MCS by various studies (Hall et al. 2005; Khanal et al. 2006; Manache and Melching 2004; Salas and Shin 1999; Smith and Goodrich 2000). FOSM methods are not capable to deal with non-normal random variables or nonlinear models, and probably results in miscalculation. On the other hand, the conventional MCS sampling methods are not computationally efficient for rare event problems. Therefore, this study proposes an efficient sampling method to reduce the computational burden arising from the conventional sampling techniques while enhancing the solution precision.

This study presents a dam overtopping evaluation model considering flood and wind events that could potentially induce dam overtopping. A maximum wind speed frequency model collected from Juang (2001) and peak floods of various recurrence intervals derived from frequency analysis, distribution types and their parameters will be presented. Frequency analyses based on the annual maximum (AMax) series and monthly maximum (MMax) series are conducted with the consideration of three distributions—Gumbel, Log-normal, and Log-Pearson type III distributions. Through the use of proposed sampling scheme, reservoir routing incorporating reservoir operation rules during flood period, wind setup, and run-up models are used to evaluate dam overtopping probability.

2 Methodology of assessing dam overtopping probability

Overtopping causes about 35% of earth dam failures according to ICOLD (1973). Dam overtopping events are triggered mostly by flood events, possibly accompanied by strong wind events. Some are caused by massive landslide into the reservoir, which generate surface water wave leading to overtopping. In this section, procedures for reservoir routing, flood frequency analysis, and proposed sampling scheme to evaluate overtopping probability of Shihmen Dam are described.

Figure 1 demonstrates the procedure of overtopping probability assessment. It involves following steps:

1. *Identifying and assessing the important factors*: The uncertainty factors considered in this study include the flood magnitude, Q, and wind speed, W. The statistical properties of each uncertainty factor will be discussed in detail.
2. *Data collection and analysis*: Flood data collected for frequency analysis include the AMax series and MMax series of flood events. The distribution parameters for random wind speed at various locations in Taiwan were determined by Juang (2001).
3. *Uncertainty analysis*: Probabilistically plausible realizations of each uncertainty factors are generated by the proposed sampling scheme which preserves their respective distributional properties.
4. *Perform reservoir routing*: The random variable sets generated in Step 3 are used in reservoir routing model that considers operation rules during flood period, wind wave setup and run-up. The model responses are then analyzed to evaluate dam overtopping probability.

A method is required to convert surface water level into overtopping probability. This study adopts on the methods used by Cheng et al. (1982) and Pohl (1999). Figure 2 demonstrates the conceptual diagram of dam overtopping probability considering the joint occurrence of wind and flood events subjected to uncertainties.

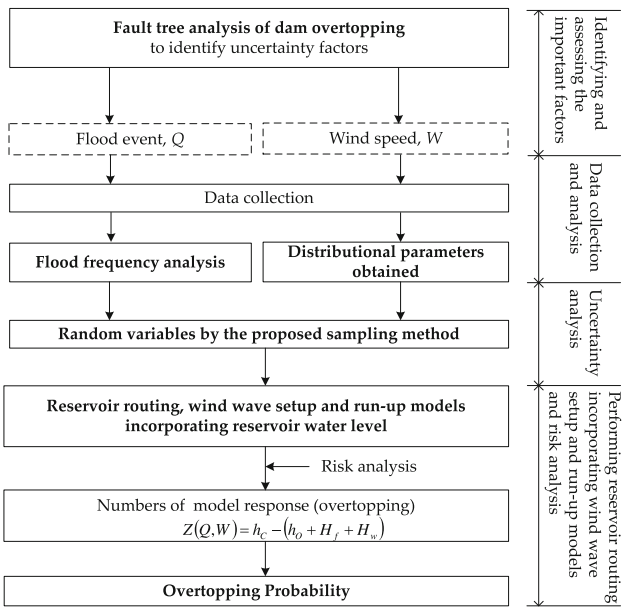

Fig. 1 Flow chart for assessing dam overtopping probability

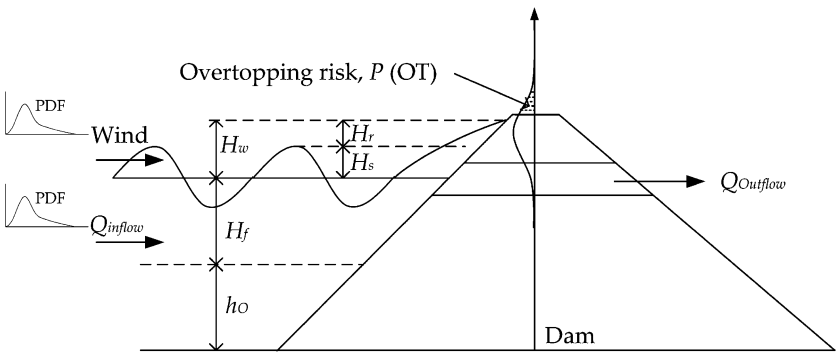

Fig. 2 Conceptual diagram of dam overtopping. H_r wind wave runup, H_s wind wave setup, H_w wind wave setup + wind wave runup, H_f surface water level raised by flood event, h_O initial reservoir water level

The general formulation associated with the sampling methods for dam overtopping probability analysis can be represented by $h_O + H_f + H_w > h_C$, where h_C is dam crest height assumed known without uncertainty; h_O is initial surface water level; and H_f and H_w are random water surface level increased by flood and wind events, respectively, in which $H_w = H_s + H_r$ with H_s being wave setup and H_r being wave run-up. Dam overtopping probability, Pr(OT), induced by the three random variables can be expressed as

$$\Pr(\mathrm{OT}) = \int_{h_O}^{\infty}\int_{h_f}^{\infty}\int_{h_w}^{\infty} f(h_O, h_f, h_w)\cdot dh_w \cdot dh_f \cdot dh_O \qquad (1)$$

where $f_{x,y,z}(\cdot)$ is the joint PDF of the three variables. Assuming that h_O, H_f, and H_w are statistically independent, Eq. 1 can be written as

$$\Pr(\mathrm{OT}) = \int_{h_O}^{\infty}\int_{h_f}^{\infty}\int_{h_w}^{\infty} f_{H_O}(h_O)\cdot f_{H_f}(h_f)\cdot f_{H_w}(h_w)\cdot dh_w \cdot dh_f \cdot dh_O \qquad (2)$$

and $f_x(x)$ is the marginal PDF of random variable X.

3 Frequency analysis

The primary object of frequency analysis is to relate the magnitude of extreme events to their frequency of occurrence through the use of probability distributions (Chow et al. 1988). Flood data observed over an extended period of time in a river system are analyzed in frequency analysis. The data are assumed to be independent and identically distributed. Furthermore, it is assumed that the floods have not been affected by natural or man-made changes in the hydrological regime in the system.

In previous related studies (Kuo et al. 2004, 2007), flood frequency analysis was conducted on the basis of AMax data. The use of AMax series may involve loss of information. For example, the second or third peak within a year may be stronger than the maximum flow in other years and yet they are ignored (Kite 1975; Chow et al. 1988). As a result, the overtopping probability could be underestimated.

In this study, the effect of using AMax and MMax flood data is investigated. Several better fit distributions in both AMax and MMax flood frequency analysis will be examined through the Anderson-Darling (AD) goodness-of-fit test. A comparison of the results based on AMax and MMax flood series will be discussed.

As for wind speed, distributional properties are adopted from Juang (2001). The distributional properties of flood and wind speed are used in the reservoir routing which incorporates wind wave setup and run-up models to evaluate the dam overtopping probability.

3.1 Flow AMax and MMax series models

The flood data collected from the Shihmen Reservoir include 38 years of records (1963–2000) in the form of daily average flow rate. To perform reservoir routing with the inflow hydrograph with a 3-day base time, the daily average records should be converted into 3-day average discharges by taking average of continuous 3-day flow rates before flood frequency analysis. The statistical properties of the 3-day flow records are listed in Table 1. Once the AMax and MMax 3-day average flow rates are obtained, frequency analysis can be carried out to estimate the flow rates of different return periods. The flow rate can be further converted into an inflow hydrograph which is comprised with a rising, a peak and a falling segments.

The AMax and MMax 3-day average flow rates are subjected to the Anderson-Darling goodness-of-fit test for Normal (N), 2-parameter Log-normal (LN), Pearson type III (P3), Log-Pearson type III (LP3), Weibull, and Gumbel distributions were tested. The results showed that Gumbel, Log-normal, and Log-Pearson type III distributions have better fit than the other candidate distributions considered herein. The test statistic values of the three candidate distributions for AMax and MMax 3-day average flow rates are listed in Table 2. It shows that the three distribution models might not be the best for all AMax series and MMax series. However, some of the results shown in Fig. 3

Table 1 Statistical properties of the flow records at Shihmen Dam

Data type	$\bar{Q}$	σ_Q	$C_{S,x}$	$\bar{Q}_y$	σ_{Q_y}	$C_{S,y}$
AMax	608.46	533.59	3.03	2.65	0.37	−0.48
MMax-May	60.26	41.28	1.64	1.69	0.30	−0.31
MMax-June	116.68	105.30	1.84	1.93	0.33	0.43
MMax-July	125.63	136.24	1.41	1.86	0.46	0.34
MMax-Aug	315.15	351.54	1.26	2.16	0.59	0.03
MMax-Sep	361.52	551.07	3.76	2.24	0.54	0.06
MMax-Oct	180.61	237.78	2.21	1.97	0.49	0.54

AMax and MMax represent the annual maximum and monthly maximum series

$\bar{Q}$ and σ_Q represent the mean and standard deviation of the observed floods in real space

$\bar{Q}_y$ and σ_{Q_y} represent the mean and standard deviation of the observed floods in log space

$C_{S,x}$ and $C_{S,y}$ represent the coefficients of skewness of the observed floods in real space and in log space

Table 2 Statistics values of probability distributions for 3-day average flow

Data type	Distribution	AD	*P*-value
AMax	LN	0.681	0.07
	Gumbel	0.32	>0.25
	LP3	0.954	0.017
MMax-May	LN	0.249	0.73
	Gumbel	0.391	>0.25
	LP3	0.26	>0.25
MMax-June	LN	0.411	0.326
	Gumbel	1.695	<0.01
	LP3	0.204	>0.25
MMax-July	LN	0.74	0.049
	Gumbel	2.863	<0.01
	LP3	0.569	0.159
MMax-Aug	LN	1.128	0.005
	Gumbel	2.867	<0.01
	LP3	1.046	0.01
MMax-Sep	LN	0.217	0.83
	Gumbel	2.246	<0.01
	LP3	0.236	>0.25
MMax-Oct	LN	1.002	0.011
	Gumbel	3.099	<0.01
	LP3	0.832	0.034

AD Anderson-Darling statistic

indicate that the three distribution models are acceptable. Hence, the three distributions are used in the proposed sampling scheme to generate floods of various frequencies and, then, convert them into inflow hydrographs for reservoir routing.

By frequency analysis of flood data, flow rates of different return periods can be estimated by

$$\hat{x}_T = \bar{x} + K_T s \tag{3}$$

where $\bar{x}$ and s are, respectively, the sample mean and standard deviation of flood data; and K_T is a frequency factor depending on the skew coefficient, probability distribution, and return period.

3.2 Wind speed frequency

The parameters of wind frequency distribution are directly adopted from Juang (2001), who collected and analyzed wind speed data of typhoons in Taiwan from 1961 to 1998. The magnitude of wind speed is not only affected by the typhoon intensity, but also affected by the terrain features and path of typhoons.

The most widely used distributions in wind speed frequency analysis are Gumbel, extreme value type II, Rayleigh, two- and three-parameter Weibull, and generalized Pareto distributions. Juang's (2001) study indicates that the Gumbel distribution has the best-fit over other candidate distribution models considered. The PDF and CDF of the Gumbel distribution are given, respectively, as

$$f(U) = a\exp\{-a(U-b) - \exp[-a(U-b)]\} \tag{4}$$

$$F(U) = \exp\{-\exp[-a(U-b)]\} \tag{5}$$

where U represents the wind speed; and a and b represent the scale and location parameters. Of all the stations considered by Juang (2001), Jujihu Station not only has a terrain most similar to that of the Shihmen Reservoir but also is geographically close to it. Hence, wind speed characteristics at this station may be comparable to those of Shihmen Reservoir. The values of parameters a and b, which represent the wind directions at different compass points at Jujihu Station, determined by Juang (2001) is then used in the wind wave setup and run-up models to evaluate the surface water level raised by the wind.

4 Determination of performance function

The failure of an engineering system can be defined as the loading on the system (L) exceeds the resistance of the system (R). The performance function of an engineering system can be described in several forms: (1) safety margin, $Z = L - R$; (2) safety factor, $Z = R/L$; or (3) safety factor in log space, $Z = \ln(R/L)$. The use of appropriate form depends on the distribution type of the performance function. Yen (1979) summarized several forms of performance function and discussed their applications to hydraulic engineering systems. Generally, safety margin is the most

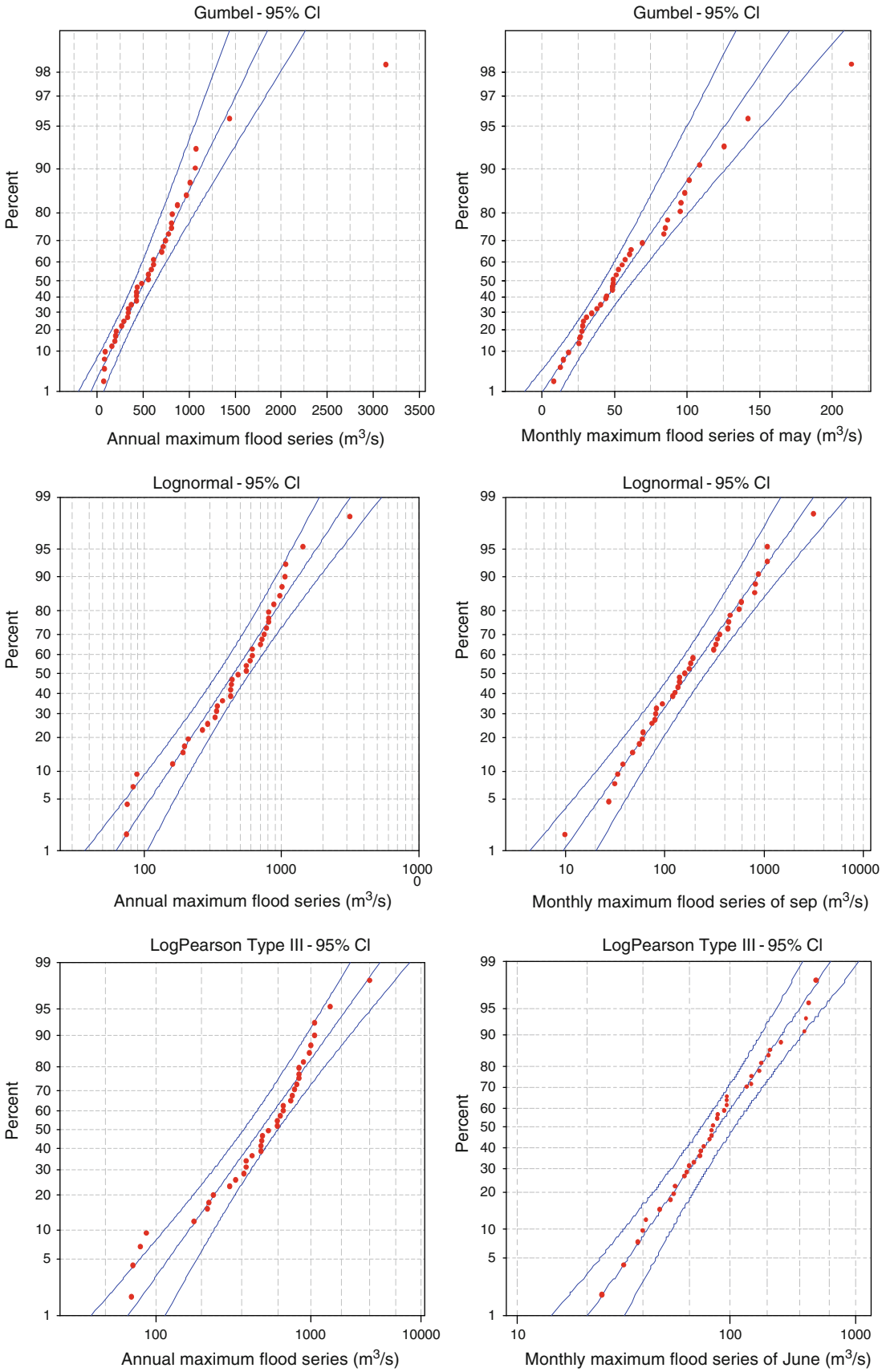

Fig. 3 Illustration of some acceptably fit distributions for flood data

used performance function form in dam overtopping analysis. The reliability of a hydraulic infrastructure can be defined

$$\alpha = \Pr[R \geq L] = \Pr[Z \geq 0] \tag{6}$$

where Pr[ ] represents the probability. Therefore, the failure probability α' can be represented as

$$\alpha' = \Pr[L > R] = \Pr[Z < 0] = 1 - \alpha \tag{7}$$

Dam overtopping can be induced by one of the following conditions: (1) induced by flood only; (2) by wind only; or (3) jointly by flood and wind. Sections 4.1–4.3 describe the performance functions appropriate to these three conditions.

4.1 Overtopping induced by flood only

Reservoir routing is modeled by the discrete form of the continuity equation:

$$\frac{I_t + I_{t+1}}{2} - \frac{O_t + O_{t+1}}{2} = \frac{S_{t+1} - S_t}{\Delta t} \tag{8}$$

where I_t, O_t, and S_t, respectively, represent reservoir inflow, outflow, and storage volume at times t; and Δt is the routing time interval.

Reservoir inflow hydrograph can be converted from the flow rate obtained by the flood frequency analysis. When using a MCS sampling method to generate peak flow rates, one needs to randomly generate a set of the frequency factors from an adopted distribution to obtain the corresponding peak flow rates. Using Eq. 8 by incorporating reservoir operation rules during flood period, one can compute the reservoir storage at any time t during a flood event. The reservoir storage at time t can be converted into the water level hydrograph using the reservoir water level-storage relation from which the highest level, $h_O + H_f$ (see Fig. 2) can be obtained. Afterwards, the performance function of dam overtopping, Z, without considering the wind induced setup and wave run-up can be described by

$$Z = g(h_C, h_O, H_f) = h_C - (h_O + H_f) \tag{9}$$

where h_C is dam crest elevation of 252.5 m; and h_O is the initial reservoir level with a fixed value of 235 m.

4.2 Overtopping induced by wind only

The magnitude of wind setup (or tide), H_S, can be estimated from the simplified Dutch's formula:

$$H_S = \frac{V_W^2 F}{1400D} \tag{10}$$

where H_S is the wind wave setup above the undisturbed water (in feet); V_W is the wind velocity (in miles/h); F is the fetch length (in miles) representing the reservoir surface distance over which the wind blows; and D is the average depth (in feet) of the reservoir along the fetch.

According to Saville et al. (1963), the wave height, H_{wh} (in feet), and wave length, L (in mile), in a reservoir are given by the following empirical equations:

$$H_{wh} = 0.34\, V_W^{1.06} F_e^{0.47} \tag{11}$$

$$L = 1.23\, V_W^{0.88} F_e^{0.56} \tag{12}$$

where F_e is effective fetch (in mile) which involves the measurements of fetch lengths from different wind directions. A general approach can be referred to the U.S. Army Corps of Engineers (1977) to determine the effective fetch by the fetch lengths from the three directions: the shore-normal, 45° to the left and 45° to the right of the shore-normal. The ratio of wave height to wave length can be estimated by

$$\frac{H_{wh}}{L} = 0.276\, V_W^{0.18} F_e^{-0.09} \tag{13}$$

With the ratio H_{wh}/L and a known embankment slope, the height of wave run-up can be estimated (Saville et al. 1963) by

$$H_r = cH_{wh} \exp[-d(H_{wh}/L)] \tag{14}$$

where c and d are coefficients for embankment slopes (Cheng et al. 1982).

The performance function of dam overtopping induced only by wind can be described by

$$\begin{aligned} Z &= g(h_C, h_O, H_W) = h_C - h_O - H_W \\ &= h_C - h_O - (H_S + H_r) \\ &= h_C - h_O - \left(\frac{V_W^2 F}{1400D} + cH_{wh} \exp\left(-d\frac{H_{wh}}{L}\right)\right) \end{aligned} \tag{15}$$

where H_W represents the reservoir water surface elevation due to the combined effect of wind wave setup and run-up.

4.3 Overtopping induced jointly by flood and wind

The performance function of dam overtopping induced jointly by flood and wind can be described by combining Eqs. 9 and 15 as:

$$\begin{aligned} Z &= g(h_C, h_O, H_f, H_W) = h_C - h_O - H_f - H_W \\ &= h_C - h_O - H_f - \left(\frac{V_W^2 F}{1400D} + cH_{wh} \exp\left(-d\frac{H_{wh}}{L}\right)\right) \end{aligned} \tag{16}$$

A probabilistic model should be considered for the loadings of wind and flood. This study adopts the probabilistic-based wind and flood model developed by Cheng et al. (1982).

5 Risk and uncertainty analyses

The main purpose of uncertainty analysis is to quantify system outputs or responses as affected by the stochastic basic parameters in the system. The selection of appropriate method for uncertainty analysis depends on the nature of the problem, including availability of information, model complexity, and type and accuracy of results desired (Tung and Yen 2005).

The uncertainty analysis methods are to quantify the distributional properties of the system responses (the performance function in this study) as affected by the uncertainty factors in the system. Let $\Pr(\mathrm{OT}|h_O, Q, W)$ represents dam overtopping probability under a fixed initial reservoir water level h_O and random peak flow rate, Q, and wind speed W. Then, dam overtopping probability can be expressed as

$$\begin{aligned}\Pr(\mathrm{OT}|h_O, Q, W) &= \Pr[Z(h_O, Q, W) < 0] \\ &= \Pr\left[h_C - H_f(h_O, Q) - H_W(W) < 0\right]\end{aligned} \tag{17}$$

where h_C, H_f, and H_W are defined previously.

The procedure used in this study for conduct uncertainty and risk assessment of dam overtopping is the combination of IS and LHS schemes. IS divides the sample space into several disadjoint sub-domains and generates random samples from the sub-domain of interest. In the context of engineering system reliability, the parts of greatest interest should be mostly at the two ends of a probability distribution. As shown in Fig. 4, the IS–LHS scheme employs IS to divide the sample space of the concerned random variable into two sub-domains, each of which is then stratified into several equal probability intervals using the LHS procedure.

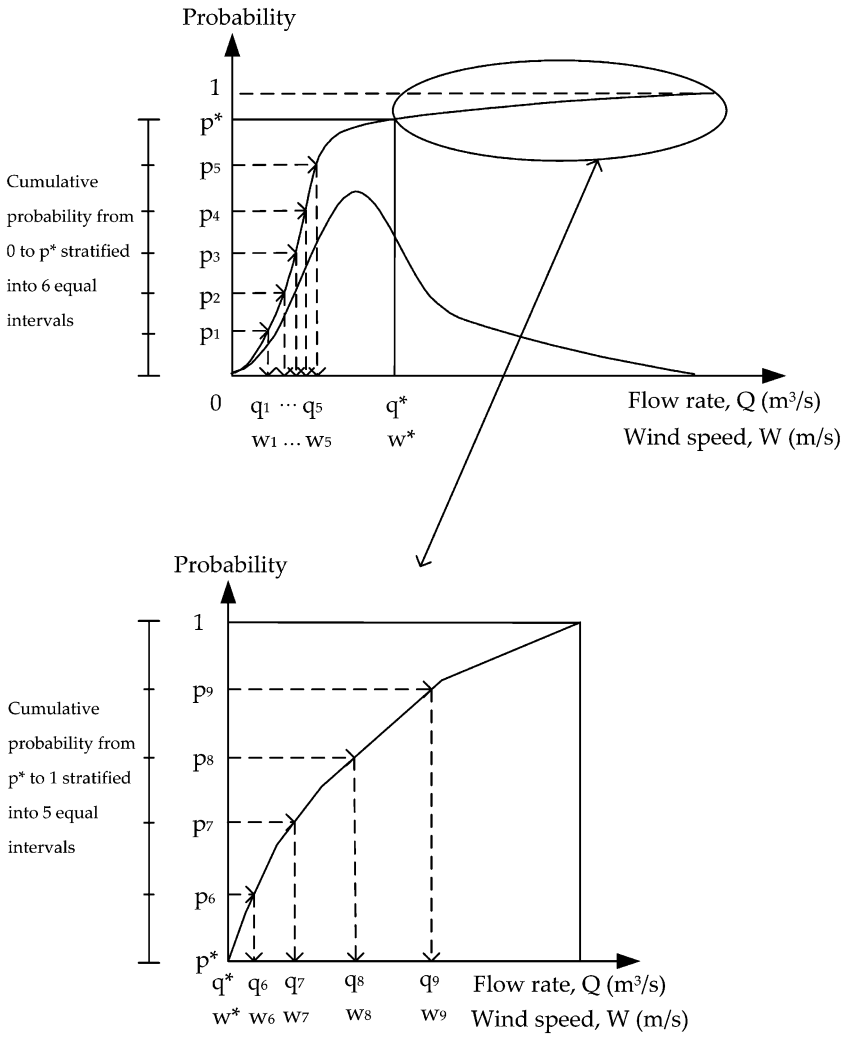

Fig. 4 Diagram of proposed IS–LHS sampling scheme

6 Case study

6.1 Shihmen Dam

Shihmen Dam, completed in 1964, is located in Shihmen Valley in the midstream of the Dahan River (see Fig. 5) in the northern part of Taiwan. The main functions of the reservoir are agricultural, industrial, and domestic water supply; hydropower generation; and flood control. Before the completion of Shihmen Dam, Typhoon Gloria hit Taiwan on September 11, 1963 which caused severe flooding in Northern Taiwan and threatened to overtop the dam. To allow for higher protection of the dam against large floods, two additional tunnel spillways were constructed in 1985. The capacity of water release facilities was increased from 10000 to 12400 m^3/s. Shihmen Reservoir has a contribution catchment of 763.4 km^2, and due to accumulation of sediment over time, its effective storage has being decreasing gradually from 309,120,000 m^3 in 1964 to 219,630,000 m^3 in 2007.

6.2 Evaluating overtopping probability of Shihmen Dam

For illustration, the initial water level is considered fixed at $h_O = 235$ m. The sample cross-correlation of the annual peak flow rate, Q, and wind speed, W, is at the low value of 0.19 (Hsu 2007). This justifies that the two random variables can be treated as independent. The dam overtopping probability of Eq. 2 can be rewritten as:

$$\Pr(\mathrm{OT}) = \int_{h_w}^{\infty}\int_{h_f}^{\infty} f_{H_f}(h_f)\cdot f_{H_w}(h_w)\cdot dh_f\cdot dh_w \tag{18}$$

A sample space defined jointly by Q and W (see Fig. 6) is divided into four sub-domains, namely, A_1, A_2, A_3, and

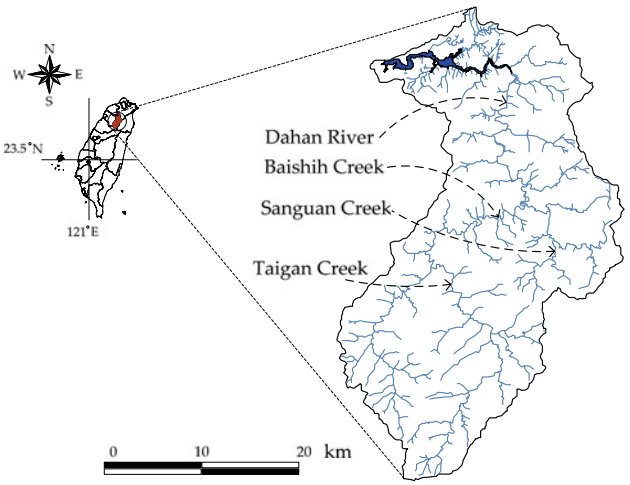

Fig. 5 Location of Shihmen Reservoir

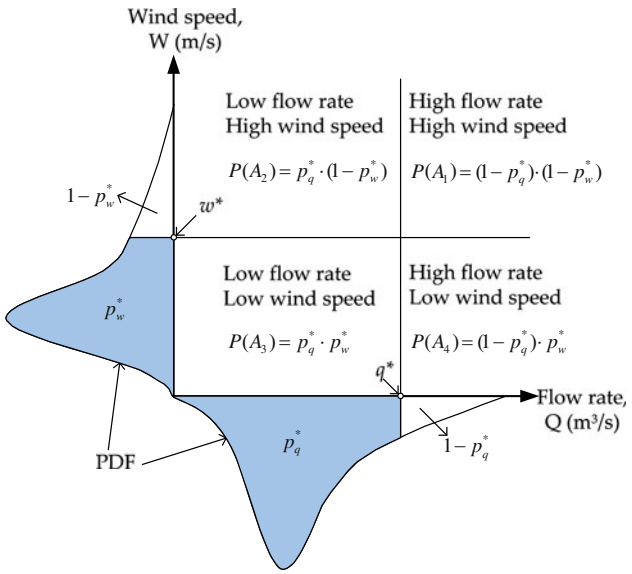

Fig. 6 Partitioning of Q–W sample space

A_4. Under the condition of statistical independence, the probability values of the four sub-domains can be calculated as:

$$\Pr(A_1) = \Pr(Q > q^*, W > w^*) = \left(1 - p_q^*\right)\cdot\left(1 - p_w^*\right) \tag{19}$$

$$\Pr(A_2) = \Pr(Q \le q^*, W > w^*) = p_q^*\cdot\left(1 - p_w^*\right) \tag{20}$$

$$\Pr(A_3) = \Pr(Q \le q^*, W \le w^*) = p_q^*\cdot p_w^* \tag{21}$$

$$\Pr(A_4) = \Pr(Q > q^*, W \le w^*) = \left(1 - p_q^*\right)\cdot p_w^* \tag{22}$$

where q^* and w^* are, respectively, the flow rate and wind speed corresponding to the cutoff points on the two probability distributions with $p_q^* = \Pr(Q < q^*)$ and $p_w^* = \Pr(W < w^*)$. In the discrete form Eq. 18 can be written as

$$\Pr(\mathrm{OT}) = \sum_{i=1}^{4}\Pr(\mathrm{OT}|A_i)\cdot\Pr(A_i) \tag{23}$$

where $\Pr(A_i)$ is the joint probability of flood and wind events defined above.

The IS–LHS scheme is then applied to generate N pairs of (Q, W) sample sets ($N = 1{,}000$ is used in this study) from each sub-domain to the dam overtopping model. A negative value of the performance function (Z) of the dam overtopping model (Eqs. 9, 15, and 16) indicates the occurrence of dam overtopping. The values of n_i, which represent dam overtopping in each sub-domain, are recorded. Then, the probability of dam overtopping in each sub-domain is expressed as n_i/N. Without considering the uncertainty of flow quantile, the total probability of dam overtopping can be evaluated by

$$\Pr(\mathrm{OT}) = \sum_{i=1}^{4} \Pr(\mathrm{OT}|A_i) \cdot \Pr(A_i) = \sum_{i=1}^{4} \left(\frac{n_i}{N}\right) \cdot \Pr(A_i) \qquad (24)$$

When dealing with the peak flow rates of sequential months in wet season (May–October) in Taiwan, one might need to take into account the correlation between MMax flood series of any two consecutive months following the approaches developed by Der Kiureghian and Liu (1985) and Chang et al. (1994). The calculation of overtopping probability considering MMax flood series can be evaluated following the procedure shown in Fig. 7.

With/without considering wind effect, the MMax peak discharges generated by the proposed sampling scheme are firstly converted into inflow hydrographs for reservoir routing which incorporates wind setup and run-up models and operation rules. From the calculated reservoir water level hydrograph the highest reservoir water levels of different months in each year can be obtained. Again, in each simulation, if there is one or more months with negatively-valued performance functions (Eqs. 9, 15, and 16), then it is considered that the dam overtopping occurs in that year. Repeating the simulation procedure, one may evaluate the annual overtopping probability by Eq. 24.

The peak discharge of a specific return period, Q_T, obtained from Eq. 3 is usually considered in practice as a single-valued quantity rather than a random variable associated with its probability distribution. The analysis further takes into account the flow quantile uncertainty associated with the estimation of μ, σ, and K_T in Eq. 3. Figure 8 demonstrates an example of flood quantile in which q_c represents the critical peak discharge beyond which dam overtopping would occur and T_c represents its corresponding return period which is also a random variable for the same reason as Q_T. If the uncertainty of estimated flow quantile is not considered, overtopping probability under the threshold peak flow rate, q_c, will be underestimated. For the estimation of sampling probability distribution of T-year flow rate, one can refer to Stedinger et al. (1993) and Rao and Hamed (2000).

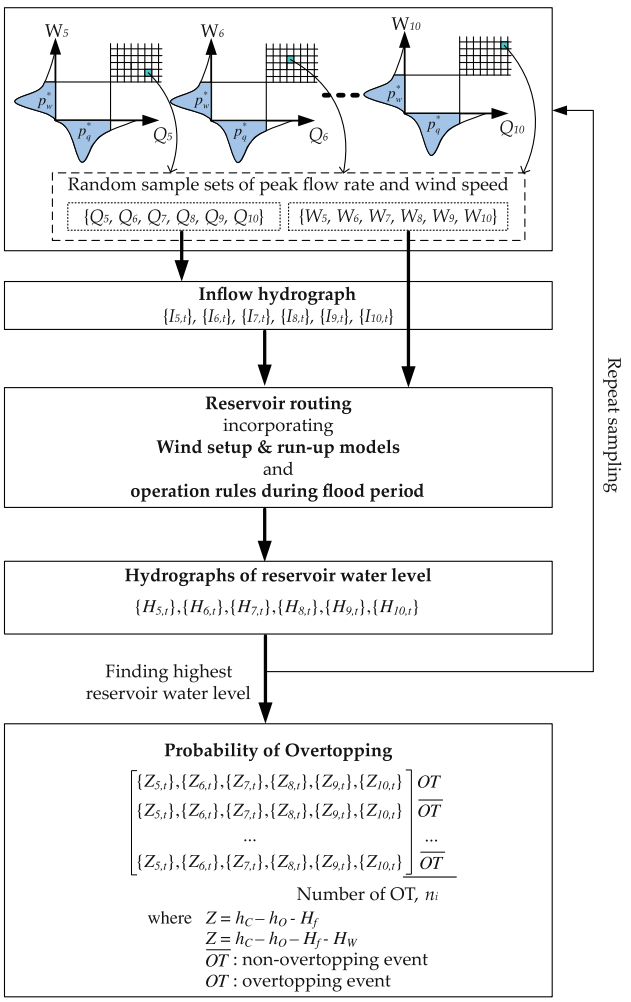

Fig. 7 Procedure of evaluating dam overtopping probability considering MMax flow samples

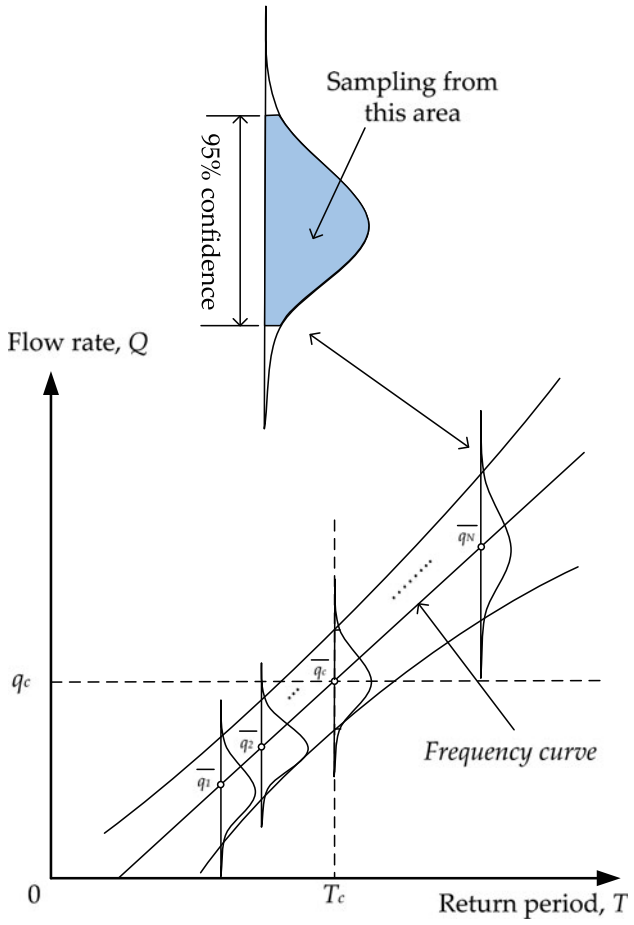

Fig. 8 Uncertainty of flow quantile of a specific return period. *Note*: q_c means the critical flow rate that can induce the dam overtopping, which corresponds to the return period of critical flow T_c

Taking into account the uncertainty inherent in parameter estimated from limited samples, the LHS method is applied to generate samples from the normal distribution within the 95% confidence interval with mean value of T-year flow rate, Q_T, and standard error, S_T, for the Gumbel (Kite 1975), Log-normal (Rao and Hamed 2000), and Log-Pearson type III (Rao and Hamed 2000) distributions given, respectively, by:

$$\text{For Gumbel:} \quad s_T = \sigma_x \left[\frac{1}{n} \left(1 + 1.1396\, K_T + 1.1\, K_T^2 \right) \right]^{1/2} \tag{25}$$

$$\text{For Log-normal:} \quad s_T = \frac{\sigma_y}{\sqrt{n}} \left(1 + \frac{u_T}{2} \right)^{1/2} \exp\left(\mu_y + u_T \sigma_y \right) \tag{26}$$

$$\text{For Log-Pearson type 3:} \quad s_T = \frac{\sigma_x}{\sqrt{n}} \left[1 + K_T C_S + \frac{K_T^2}{2} \left(\frac{3C_S^2}{4} + 1 \right) + 3K_T \frac{\partial K_T}{\partial C_S} \left(C_S + \frac{C_S^3}{4} \right) + 3 \left(\frac{\partial K_T}{\partial C_S} \right)^2 \left(2 + 3C_S^2 + \frac{5C_S^4}{8} \right) \right]^{1/2} \tag{27}$$

where σ_x and σ_y are, respectively, the standard deviation of flow rates in the original and log-space; C_S is the coefficient of skewness; K_T is the frequency factor; u_T is the standard normal variate corresponding to an exceedance probability $1/T$.

The LHS method is applied to produce random samples from the normal distribution with mean value of T-year flow rate and standard error determined by Eqs. 25–27. The sample size M used in this study is 50. Then, the dam overtopping probability considering random T-year peak flow rate is given by

$$\Pr(\text{OT}) = \sum_{i=1}^{4} \left(\frac{m_i}{N \cdot M} \right) \cdot \Pr(A_i), \quad i = 1, 2, 3, 4 \tag{28}$$

where m_i, represent the number of dam overtopping in each sample sub-domain when considering flow quantile uncertainty.

The overtopping probability under the MMax condition can be validated by system reliability assessment in which failure of each month is regarded as component failure with the corresponding exceedance probability, P_e, as the component failure probability. Thus, the overtopping probability considers MMax without taking account the wind effects and flow quantile uncertainty is bounded by the following equation:

$$\max P_{e_i} \le \Pr(\text{OT}) \le 1 - \prod_{i=5}^{10} (1 - P_{e_i}), \quad i = 5, 6, \ldots, 10 \tag{29}$$

where P_{e_i} represents the probability exceeding the critical peak flow rate for month i in the wet season (May–October). In the case of uncorrelated consecutive MMax series, the dam overtopping probability would approach to the upper limit of Eq. 29.

6.3 Results

The case study follows the procedure in Fig. 1 considering the frequency analysis models of AMax and MMax series for dam overtopping probability evaluation. The proposed IS–LHS scheme was applied to generate 1,000 sets of peak flow and wind speed, without considering the uncertainty associated with T-year flood. When considering the sampling error associated with flood quantiles, the generated sample size is increased to 1,000 × 50 to produce T-year flow rate samples based on its mean and standard error.

The reservoir routing incorporating wind wave setup and run-up models is applied to simulate the reservoir water level hydrograph with a fixed initial water level at 235.0 m under the flood and wind speed sample sets produced by the proposed sampling scheme. The resulting dam overtopping probabilities following Eqs. 19–24 are shown in Table 3. Figures 9 and 10 illustrate the dam overtopping probability evaluated by different distribution models.

The results reveal that dam overtopping probability under the Gumbel distribution is much smaller than that under other alternative distributions considered. This can be explained from Fig. 11 which shows that the Gumbel distribution has the lowest probability (P_e) exceeding the critical peak rate of 23615 m^3/s if only taking account flood events. This indicates that assuming observed floods to follow the Gumbel distribution will result in lower dam overtopping probability. Moreover, Figs. 9 and 10 also show that dam overtopping probability considering MMax flood series is generally greater than that of the AMax series, except the Gumbel distribution.

With MMax series, Figs. 12, 13, and 14 show P_e-curves associated with the three distribution models considered reveal that some P_e values at the critical peak flow rate are smaller than but close to those using AMax data. Thus, according to Eq. 29, dam overtopping probability obtained from using MMax flood data series is inevitably greater than that using AMax flood data, except for the Gumbel distribution because its relatively smaller P_e values under MMax data than under Amax data. This reveals that the use of AMax series may involve loss of information and consequently underestimate dam overtopping probability.

Taking into account the fact that flow rates (q_{1MM} and q_{2MM} in Fig. 15) under the MMax flood series should be less than or equal to those (q_{1AM} and q_{2AM}) of the AMax series model at a same P_e value, the study further allows the sampled flow rates of MMax series follow the monthly P_e curve in the region from 0 to p^* and the annual P_e curve from p^* to 1. For the monthly P_e curves that have no

Table 3 Dam overtopping probability considering flood events following Gumbel distribution based on annual maximum flood series

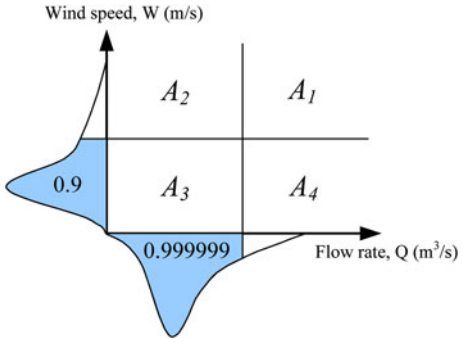

Sub-domain	Pr(OT|A_i)	Pr(A_i)	Pr(OT ∩ A_i)
(a) Consider flood and wind without considering flood quantile uncertainty			
1	1.175E−01	1.000E−07	1.180E−08
2	0.000E+00	1.000E−01	0.000E+00
3	0.000E+00	9.000E−01	0.000E+00
4	4.670E−02	9.000E−07	4.203E−08
			5.378E−08
(b) Consider flood only without considering flood quantile uncertainty			
1	1.150E−02	1.000E−07	1.150E−09
2	0.000E+00	1.000E−01	0.000E+00
3	0.000E+00	9.000E−01	0.000E+00
4	1.140E−02	9.000E−07	1.026E−08
			1.141E−08
(c) Consider flood and wind and flood quantile uncertainty			
1	1.426E−01	1.000E−07	1.426E−08
2	0.000E+00	1.000E−01	0.000E+00
3	0.000E+00	9.000E−01	0.000E+00
4	6.164E−02	9.000E−07	5.548E−08
			6.974E−08
(d) Consider flood only and flood quantile uncertainty			
1	1.500E−02	1.000E−07	1.500E−09
2	0.000E+00	1.000E−01	0.000E+00
3	0.000E+00	9.000E−01	0.000E+00
4	1.500E−02	9.000E−07	1.350E−08
			1.500E−08

Pr(OT|A_i) represents overtopping probability conditional on A_i

intersection with the annual P_e curve (Figs. 12, 14), the sample flow rates will still follow the lower of the two curves. With this condition imposed, the overtopping probability under the MMax flood series drops down to a more reasonable level.

The use of P_e in this study has two purposes: (1) to understand the occurrence rates of overtopping if only considering the flood events under different distributions models; and (2) to explain the overtopping probability values obtained by the proposed methodology. Table 4 shows that the P_e values corresponding to the critical peak flow rate can be treated as the values of dam overtopping probability if only flood events are accounted for. By Eq. 29, these P_e values can further determine the lower and upper bounds of the dam overtopping probability without considering flood quantile uncertainty.

Table 4 also shows that the values of dam overtopping probability from using MMax flood data with the Log-normal and Log-Pearson 3 distributions all fall within the bounds, except the Gumbel distribution with a relatively

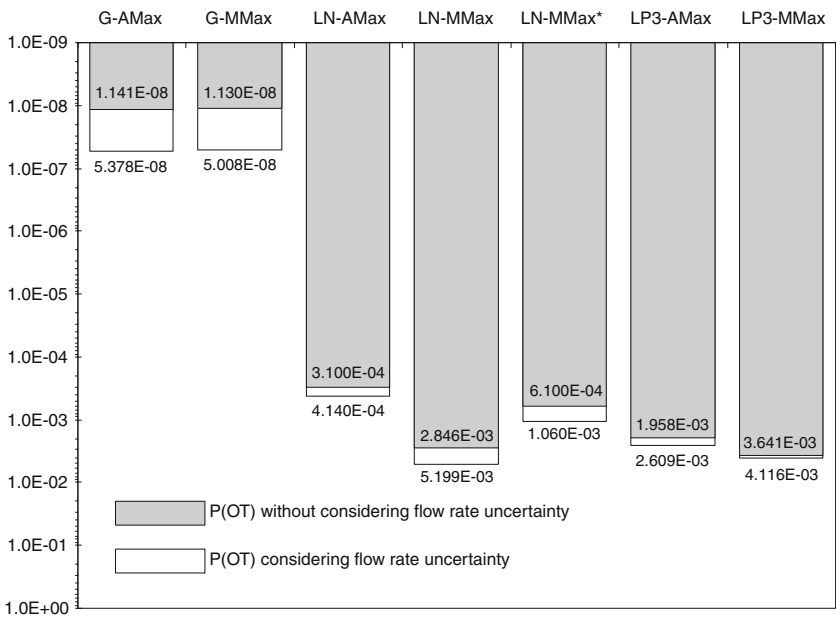

Fig. 9 Dam overtopping probability without considering estimated flood quantile uncertainty. *Note*: G, LN, and LP3 represent the Gumbel, Log-normal, and Log-Pearson type III distributions, AMax and MMax represent the annual maximum and monthly maximum series models

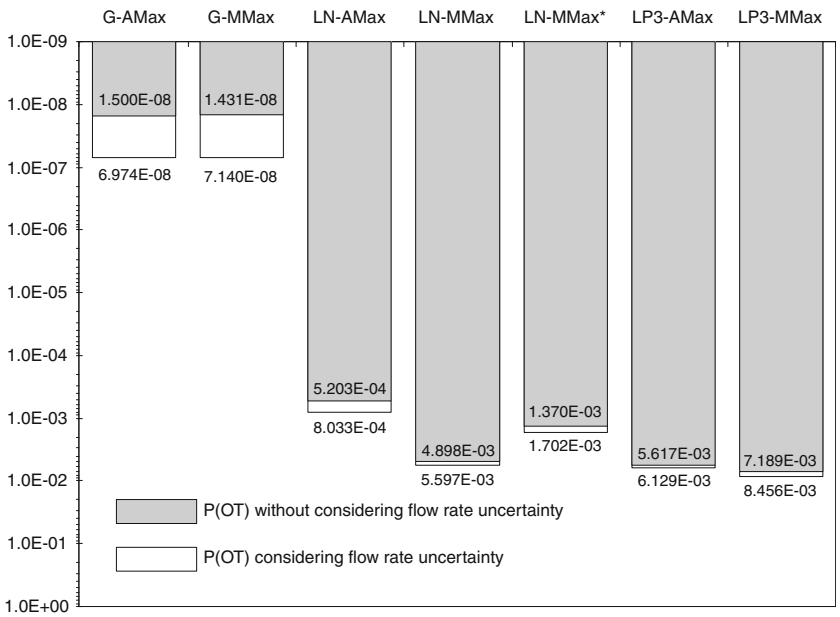

Fig. 10 Dam overtopping probability considering flood quantile uncertainty. *Note*: G, LN, and LP3 represent the Gumbel, Log-normal, and Log-Pearson type III distributions, AMax and MMax represent the annual maximum and monthly maximum series models

smaller monthly P_e values (except of September), the upper and lower bounds are found to be identical. Moreover, the values of dam overtopping probability Pr(OT) from using MMax flood data with the three distributions are closer to their upper bounds, which support the use of MMax flood series to be uncorrelated in this case study.

Considering the flow quantile uncertainty, dam overtopping probability was found to be two times, on the average, greater than without accounting for the uncertainty of flow quantiles. Thus, evaluation of dam overtopping probability without considering the flow quantile uncertainty could underestimate its potential risk.

In this study, the values of dam overtopping probability were evaluated on the basis of the three adopted distributions herein and their average values given in Table 5. With flow quantile uncertainty taken into account, dam overtopping probability due to flood only is in the range $2.046–2.853 \times 10^{-3}$ whereas due to both flood and wind $2.311–3.386 \times 10^{-3}$. On the average, Table 5 indicates that dam overtopping probability was found to be 113–119% higher than that without considering the wind effect. For reservoir watersheds prone to have strong wind, wind effect should be taken into account in dam overtopping risk assessment.

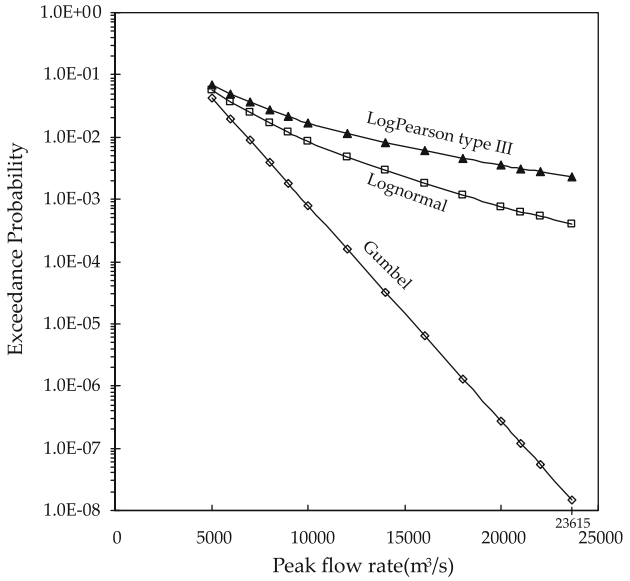

Fig. 11 Exceedance probability curves based on AMax flood series

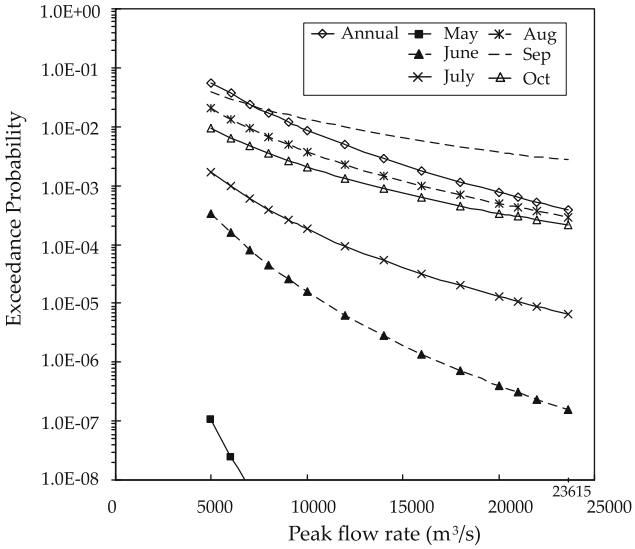

Fig. 13 Log-normal exceedance probability curves based on AMax and MMax flood series

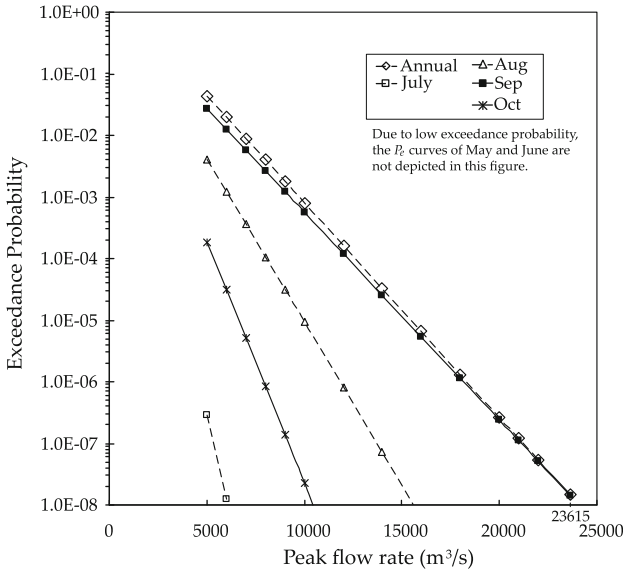

Fig. 12 Gumbel exceedance probability curves based on AMax and MMax flood series

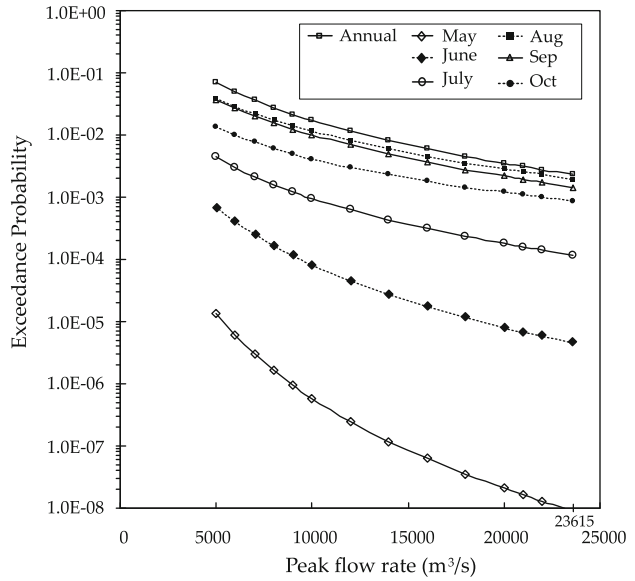

Fig. 14 Log-Peaeson 3 exceedance probability curves based on AMAx and MMax flood series

7 Summaries and conclusions

The study developed a framework for analyzing overtopping probability considering uncertainties associated flood and wind speed. The procedure involves frequency analysis of floods and wind speeds, reservoir routing considering reservoir operation, and incorporation of wind wave setup and run-up to calculate the reservoir water level hydrographs. The proposed sampling scheme combining IS and LHS was applied to replicate the flood and wind speed samples to risk analysis of dam overtopping. The IS–LHS scheme has been shown to perform efficiently for problems involving low probability/high consequence events.

Overtopping probability was evaluated by using AMax and MMax flood series over three distributions: Gumbel, Log-normal, and Log-Pearson 3. Dam overtopping probabilities obtained from using MMax flood data series was found to be higher than those from using AMax flood data, except the Gumbel distribution, because its right-end tail probability is much smaller than that of the other two distributions. In dam safety engineering, right-end tail probabilities of various distribution types influence dam designs or the safety assessment of existing dams. Therefore,

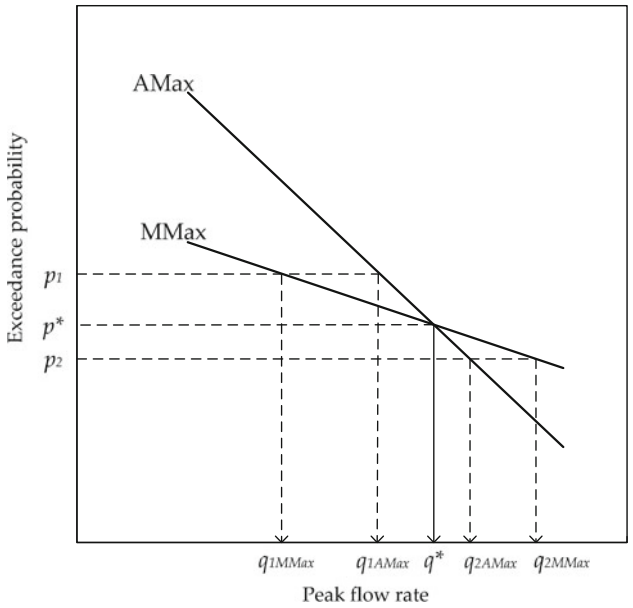

Fig. 15 Exceedance probability curves of AMax and MMax flood series

Table 4 Lower and upper bounds of dam overtopping probability under AMax and MMax flood series before adjustment of sampled monthly flow rate

Month	Exceedance probability at the critical flow rate, P_e			
	Gumbel	LP3	LN	LN[a]
May	0.000E+00	9.091E−09	0.000E+00	0.000E+00
June	0.000E+00	4.456E−06	1.542E−07	1.542E−07
July	0.000E+00	1.181E−04	6.570E−06	6.570E−06
Aug	1.098E−12	1.948E−03	2.883E−04	2.883E−04
Sep	1.440E−08	1.455E−03	2.694E−03	3.932E−04
Oct	0.000E+00	8.760E−04	2.116E−04	2.116E−04
Lower bound	1.440E−08[b]	1.948E−03	2.694E−03	3.932E−04
Pr(OT)	1.141E−08	3.641E−03	2.846E−03	6.100E−04
Upper bound	1.440E−08	4.396E−03	3.199E−03	8.995E−04

[a] Represents that the exceedance probability after flow rate adjustment if sampled peak flow rate under MMax flood series is greater than that under AMax flood series

[b] Represents the lower bound given by Gumbel distribution with a relatively smaller monthly P_e values (except of September), the upper and lower bounds are found to be identical

determining plausible distribution model to use is an important issue in rare event problems.

Wind speed could have potential impact to dams, especially for reservoirs in areas prone to typhoons or hurricanes. Results revealed that dam overtopping probability was found to be 113–119% greater than without considering the wind effect. Sinotech (1998) found that the reservoir water level could potentially increase 1.69 m because of strong wind. However, Sinotech did not consider the uncertainty of wind speed, or additional failure probability induced by wind effect.

Table 5 Average overtopping probability considering flow quantile uncertainty

Model	Overtopping probability	
	Flood and wind	Flood only
AMax	2.311E−03	2.046E−03
MMax	3.386E−03	2.853E−03

AMax and MMax represent annual maximum and monthly maximum flood series

Pr(OT) represents dam overtopping probability

The proposed sampling scheme that combines IS and LHS performed efficiently for rare event simulations. This method reduces the computational burden of the conventional simple random sampling methods while preserving solution precision.

The purpose of using a fixed initial reservoir water level in this study was to explain the model outcomes through the exceedance probability for critical discharge using system reliability. As investigated by Kuo et al. (2007), initial reservoir water level is one of the importance factors affecting the dam overtopping. Thus, the random features of the initial reservoir water level should be properly taken into account in the further study.

Reservoir operation rules can affect the reservoir water level during flood events. For conservatism, reservoir water level can be lowered by a conservative operation, but low water level would subsequently impact the economic activities in the dry season that follows. Conversely, for a less conservative operation rule would result in a higher, water level rendering in higher danger in seepage and overtopping probability. A study on this trade-off problem by adjusting the reservoir operation rules is useful.

The study did not consider the seismically-induced wave. However, Sinotech (1998) indicated that there might potentially have 0.76 m of seismically-induced wave for Shihmen Reservoir by Sato formula with 0.18 g of horizontal acceleration with a full-reservoir water level. The value of seismic-induced wave height was evaluated deterministically. Furthermore, this simplified assumption might overrate wave height without considering real water level and ground acceleration. For completeness, a practical approach to evaluating the seismically-induced wave in a reservoir is desired.

Acknowledgments This study was carried out under the project (Grant No. NSC 92-2211-E-002-255) by the institutional and financial support from National Science Council (NSC), Taiwan. The first author would like to acknowledge the scholarship (Application No. 0499862) sponsored by the Hong Kong University of Science and Technology for the opportunity to pursue this research there.

References

Afshar A, Marino MA (1990) Optimizing spillway capacity with uncertainty in flood estimator. J Water Resour Plan Manag 116(1):74–81

Askew JA, Yeh WG, Hall AH (1971) Use of Monte Carlo techniques in the design and operation of a multipurpose reservoir system. Water Resour Res 7(4):819–826

Chang CH, Tung YK, Yang JC (1994) Monte Carlo simulation for correlated variables with marginal distributions. J Hydraul Eng ASCE 120(2):313–331

Cheng ST (1993) Statistics of dam failure. In: Yen BC, Tung YK (eds) Reliability and uncertainty analysis in hydraulic design. ASCE, New York, pp 97–105

Cheng ST, Yen BC, Tang WH (1982) Overtopping probability for an existing dam. Civil Engineering Studies, Hydraulic Engineering Series No. 37. University of Illinois at Urbana-Champaign, Urbana

Chow VT, Maidment DR, Mays LW (1988) Applied hydrology. McGraw-Hill International Book Co., New York

Der Kiureghian A, Liu PL (1985) Structural reliability under incomplete probability information. J Eng Mech ASCE 112(1): 85–104

Haimes YY (1998) Risk modeling, assessment and management. Wiley, New York

Hall JW, Tarantola S, Bates PD, Horritt MS (2005) Distributed sensitivity analysis of flood inundation model calibration. J Hydraul Eng ASCE 131(2):117–126

Hsu YC (2007) Integrated risk analysis for dam safety. Ph.D. dissertation, Graduate Institute of Civil Engineering, National Taiwan University

Hsu YC, Lin JS, Kuo JT (2007) A projection method for validating reliability analysis of soil slopes. J Geotech Geoenviron Eng ASCE 133(6):753–756

International Commission on Large Dams (ICOLD) (1973) Lessons from dam incidents (reduced edition). ICOLD, Paris

Juang YS (2001) A study on wind speed probabilistic distributions in Taiwan. M.S. thesis, National Central University, Taiwan (in Chinese)

Karlsson PO, Haimes YY (1988a) Risk-based analysis of extreme events. Water Resour Res 24(1):9–20

Karlsson PO, Haimes YY (1988b) Probability distributions and their partitioning. Water Resour Res 24(1):21–29

Karlsson PO, Haimes YY (1989) Risk assessment of extreme events: application. J Water Resour Plan Manag 115(3):299–320

Khanal N, Buchberger SG, McKenna SA (2006) Distribution system contamination events: exposure, influence, and sensitivity. J Water Resour Plan Manag ASCE 132(4):283–292

Kite GW (1975) Confidence limits for design events. Water Resour Res 11(1):48–53

Kuo JT, Hsu YC, Wu JD, Yeh KC, Lin GI (2004) Determining optimal interval for dam safety inspection: Shihmen reservoir as a case study. In: Proceedings of the 6th international conference on hydroscience and engineering (ICHE-2004), Brisbane, Australia, paper on CD-ROM, Abstract, pp 457–458

Kuo JT, Yen BC, Hsu YC, Lin HF (2007) Risk analysis for dam overtopping—Feitsui reservoir as a case study. J Hydraul Eng 133(8):955–963

Kuo JT, Hsu YC, Tung YK, Yeh KC, Wu JD (2008) Dam overtopping risk considering inspection program. Stoch Environ Res Risk Assess 22(3):303–313

Kwon HH, Moon YI (2006) Improvement of overtopping risk evaluations using probabilistic concepts for existing dams. Stoch Environ Res Risk Assess 20(4):223–237

Langseth DE, Perkins FE (1983) The influence of dam failure probabilities on spillway analysis. In: Proceedings of the conference on frontiers in hydraulic engineering, ASCE, pp 459–464

Manache G, Melching CS (2004) Comparison of risk calculation methods for a culvert. J Water Resour Plan Manag ASCE 130(3): 232–242

McKay MD (1988) Sensitivity and uncertainty analysis using a statistical sample of input values. In: Ronen Y (ed) Uncertainty analysis. CRC Press, Inc., Boca Raton, pp 145–186

Meon G (1992) Overtopping probability of dams under flood load. In: Kuo JT, Lin GF (eds) Stochastic hydraulic '92. Proceedings of the 6th international symposium. National Taiwan University, Taiwan, pp 99–106

National Research Council (1988) Committee on techniques for estimating probabilities of extreme floods, methods and recommended research. National Academy Press, Washington, DC

Pohl R (1999) Estimation of the probability of hydraulic-hydrological failure of dams. In: Kuo JT, Yen BC (eds) Risk analysis in dam safety assessment. Water Resources Publications, LLC, Highlands Ranch, pp 143–157

Rao AR, Hamed KH (2000) Flood frequency analysis. CRC Press, LLC, Boca Raton

Salas JD, Shin HS (1999) Uncertainty analysis of reservoir sedimentation. J Hydraul Eng ASCE 125(4):339–350

Saville T Jr, McClenton EW, Cochran AL (1963) Freeboard allowance for waves in inland reservoirs. Transactions ASCE 128(4): 195–226

Sinotech Engineering Consultants (1988) The first dam safety thorough inspection and assessment on Shihmen Dam. A report of Sinotech Engineering Consultants submitted to Northern Region Water Resources Office, Water Resources Bureau (WRB), Ministry of Economic Affairs, Taiwan (in Chinese)

Smith RE, Goodrich DC (2000) Model for rainfall excess patterns on randomly heterogeneous areas. J Hydrol Eng ASCE 5(4): 355–362

Stedinger JR, Vogel RM, Foufoula-Georgiou E (1993) Chapter 18: frequency analysis of extreme events. In: Maidment D (ed) Handbook of hydrology. McGraw-Hill International Book Co., New York

Tung YK, Mays LW (1981) Risk models for flood levee design. Water Resour Res 17(4):833–841

Tung YK, Yen BC (2005) Hydrosystems engineering reliability assessment and risk analysis. McGraw-Hill International Book Co., New York

US Army—Coastal Engineering Research Center (1977) Shore protection manual (3rd ed). US Government Printing Office, Washington, D.C., Multipagination

Von Thun JL (1987) Use of risk-based analysis in making decisions on dam safety. In: Duckstein L, Plate E (eds) Engineering reliability and risk in water resources. M Nijhoff, Dordrecht

Yeh KC, Tung YK (1993) Uncertainty and sensitivity analyses of pit-migration model. J Hydraul Eng ASCE 119(2):262–283

Yen BC (1979) Safety factor in hydrologic and hydraulic engineering design. In: McBean EA, Hipel KW, Unny TE (eds) Reliability in water resources management. Water Resources Publications, Highlands Ranch, pp 389–407